Synthesis and structural properties of Aza[n]helicene platinum complexes: control of *cis* and *trans* stereochemistry

Daniele Mendola,[a,b] Nidal Saleh,[a] Nora Hellou,[a] Nicolas Vanthuyne,[c] Christian Roussel,[c] Loïc Toupet,[a] Franca Castiglione,[b] Federica Melone,[d] Tullio Caronna,[d] Francesca Fontana,[d] Javier Marti-Rujas,[e] Emilio Parisini,[e] Luciana Malpezzi,[b] Andrea Mele[b,] and Jeanne Crassous[a,*]*

[a] Sciences Chimiques de Rennes UMR 6226 - Institut de Physique de Rennes UMR 6251, CNRS-Université de Rennes 1, Campus de Beaulieu, 35042 Rennes Cedex, France
E-mail: jeanne.crassous@univ-rennes1.fr

[b] Dipartimento di Chimica Materiali e Ingegneria Chimica. ‘‘Giulio Natta’’, Politecnico di Milano, Piazza L. da Vinci 32 , 20133 Milano, Italy.

[c] Aix-Marseille Univ, Centrale Marseille, CNRS, iSm2, UMR 7313, 13397, Marseille, France.

[d] INSTM R.U. and Dipartimento di Ingegneria e Scienze Applicate. Università di Bergamo Viale Marconi 5, 24044 Dalmine (Bergamo), Italy

[e] Center for Nano Science and Technology@Polimi, Istituto Italiano di Tecnologia, Via Pascoli 70/3, 20133 Milano, Italy.

KEYWORDS: Helicenes, Platinum, *Cis*/*Trans* isomerism, Chirality

Abstract

The synthesis and the structural characterization of azahelicene platinum complexes obtained from *cis*-$PtCl_2(NCEt)(PPh_3)$ and from ligands that differ both in terms of the position of the N atom and the number of fused rings, is reported. These square planar complexes of general formula $PtCl_2$(**nHm**)(PPh_3) (n = 4,5, m = 5,6) display mainly a *cis* configuration. However, by X-ray crystallographic analysis we show that for both $PtCl_2$(**4H6**)(PPh_3) and $PtCl_2$(**5H6**)(PPh_3) there is a chirality control of the *cis*-*trans* stereochemistry. Indeed, while starting from a racemic mixture of aza[6]helicene, Pt complexes with a *cis* configuration are invariably obtained, the more thermodynamically stable *trans* isomers are formed when using enantiopure ligands. We further corroborated these results by NMR analysis in solution.

Introduction

Helicenes are a class of non-planar, polycyclic aromatic compounds whose helical backbone, formed by a variable number of ortho-fused benzene or other aromatic rings, renders them intrinsically chiral despite the absence of any chiral center.[1] The extended π-conjugation of these systems explains some of their most important physical-chemical properties, including their high chiroptical properties and redox activity.[1a,b,h,i] These systems generally exhibit larger intersystem crossing rates and larger magnetic dipole moments than their planar analogs. Owing to the long lifetime of their triplet state and to their tendency to form π-π stacking, these compounds may be particularly useful as building blocks in materials for optoelectronic applications.[1b,h,i] In

particular, helicene/transition metal derivatives have recently been described in the literature as promising candidates in a variety of light emitting and sensing devices.[1h] The photoluminescence and chiroptical properties of helicenes combined with the visible light emission of transition metals are in fact very attractive features of their complexes due to the strong UV absorbance of the ligand and the possibility of energy transfer to the metal ion. Moreover, the transmission of chirality to transition metal complexes may allow the design of chiral luminescent materials, enantioselective sensors, chiroptical switches, and magnetochiral compounds.[2] Helicene derivatives have also been extensively tested for their chiral selectivity in DNA binding.[1b] Moreover, possible roles of these compounds in the context of different biomedical and biotechnological applications such as drug development and biosensing have been identified.[1b,3] Another important aspect is the new reactivity features that may originate from the different solubility properties of racemates and pure enantiomers, as recently demonstrated by some of us.[4,5] Therefore, there is considerable interest in the structural diversity of helicene-based coordination complexes and in the control of their supramolecular self-assembly properties via crystal engineering approaches.

Herein, we report the synthesis of aza[n]helicene/platinum complexes of general formula Cl_2Pt(**nHm**)(PPh_3) (**nHm**: *n*-aza[m]helicene, *n* = 4, 5, m = 5, 6), displaying either a *cis* or a *trans* configuration (Scheme 1). Five of these complexes were characterized by X-ray crystallography. Interestingly, they all displayed different packing arrangements. The tendency of the helicene ligand to form π-π stacking and the ability of the platinum complexes to form hydrogen bonds involving the chlorine atoms allow for the formation of intramolecular and intermolecular stabilizing interactions. Finally, after our first serendipitous discovery that starting from either racemic mixtures or enantiopure forms of the 4-aza[6]helicene ligand (**4H6**) can affect the

cis/*trans* stereochemistry of the resulting Pt complex,[4] we set out to investigate whether other chiral ligands such as **5H6** would display the same feature.

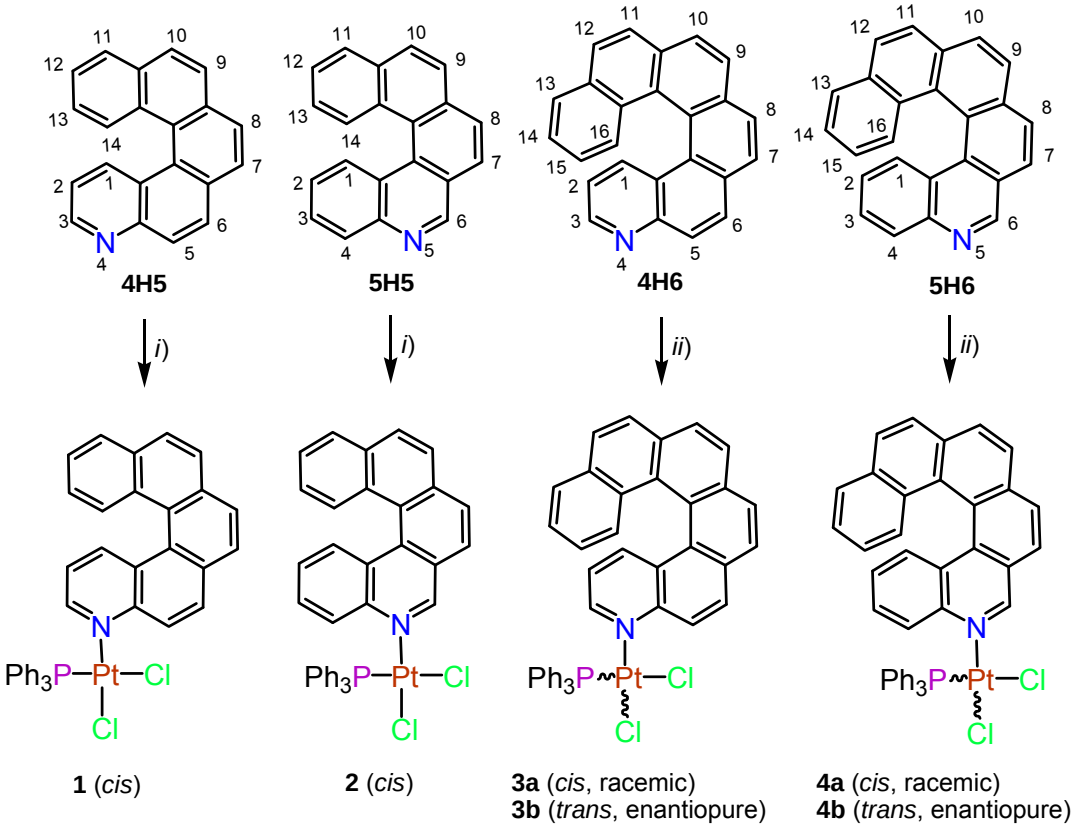

Scheme 1. Molecular structures and atom numbering for ligands **4H5**, **5H5**, **4H6** and **5H6** and for their corresponding Pt complexes **1** – **4** (**a** and **b** stands for *cis* and *trans* stereochemistry). *cis*-$PtCl_2(NCEt)(PPh_3)$ **5a**, *i*) Propionitrile, 1-4 days, RT. *ii*) Toluene, 24 hrs, reflux.

Results and Discussion

Cis Pt-complexes of aza[5]helicenes

Inspired by the interesting properties revealed by the complex between Pt and 4-aza[6]helicene,[4] we carried out the synthesis and the structural characterization of a number of Pt complexes of aza[5]helicene and aza[6]helicene ligands with N atom in different positions within the fused ring system (positions 4 and 5). At first, the relatively small 4- and 5-aza[5]helicenes were tested as ligands.[6] Our first attempt to synthesize these aza-helicene/platinum complexes starting from $PtCl_2(NCR)_2$, which is generally recognized as a good starting material,[7] did not result in the desired products but in a complex mixture. However, an efficient strategy to synthesize aza-helicene platinum complexes **1** and **2** was later developed, consisting in the substitution of the nitrile group in the *cis*-$PtCl_2(NCEt)(PPh_3)$ complex (**5a)** by the 4- or 5-aza[5]helicene ligands in propionitrile at room temperature (RT) and under continuous stirring (Scheme 2).[$] Complexes **1** and **2** were obtained from **4H5** and **5H5** respectively in moderate to good yields (Scheme 1). The ^{31}P NMR of **1** and **2** showed one signal at 3.1 ppm, with ^{195}Pt-^{31}P coupling constants of 3660-3670 Hz (see Supporting Information, SI). These complexes were also characterized by ^{195}Pt NMR which showed doublets at -3625 and -3522 ppm for **1** and **2,** respectively, with the same $J(^{195}Pt$-$^{31}P)$ coupling constants. Moreover, the aza[5]helicenes ^1H NMR chemical shifts undergo several modifications upon coordination to the $PtCl_2(PPh_3)$ moiety. For example, in complex **1**, the H5 proton of the **4H5** moiety undergoes a 1.4 ppm down-field shift upon coordination. Similarly in complex **2**, the H4 proton of the **5H5** moiety undergoes a 1.4 ppm down-field shift. In addition, the hydrogen H6 proton in the complex **2** shows a coupling constant of 4 Hz that is absent in the free ligand, and which is assigned as a $^4J_{H\text{-}P}$

coupling. Finally, the ESI mass spectrometry of both complexes **1** and **2** afforded a peak at m/z 813.2 corresponding to the cationized $[PtCl(\mathbf{nH5})(PPh_3)CH_3CN]^+$ (see SI).

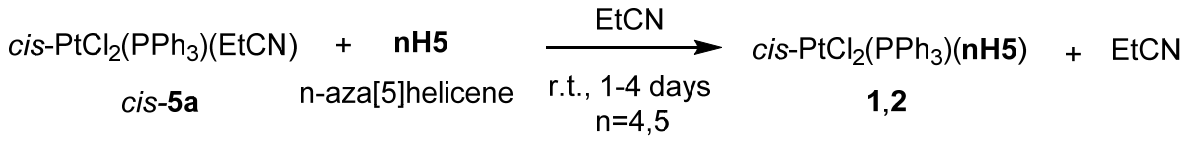

Scheme 2. Synthesis of *cis* platinum complexes **1** and **2** from **4H5** and **5H5** ligands.

Medium size single crystals of complexes **1** and **2** suitable for X-ray structural studies were obtained by slow evaporation at RT. Complex **1** crystallizes in the triclinic space group *P*-1, with one *cis*-$PtCl_2$(**4H5**)(PPh_3) molecule and one solvent molecule (dichloromethane) in the asymmetric unit. Owing to the presence of an inversion center, two molecules with opposite *M* and *P* handedness for the 4-aza[5]helicene ligand are present in the unit cell. In each complex **1**, the platinum center is coordinated by two chlorine ligands, one 5-aza[6]helicene ligand and one PPh_3 (Figures 1 and 2). The molecule shows the typical square planar geometry of platinum(II) complexes with a slight distortion from the ideal 90° arrangement (the N4-Pt-P and N4-Pt-Cl1 angles are 94.2(3)° and 87.1(3)°, respectively) presumably due to steric hindrance of the ligand. However, the Pt atom and its four coordinated atoms are quite coplanar (out of plane distortion ca. 2°). Furthermore, the distance between the platinum and the chlorine atom *trans* to the phosphine (Pt-Cl1: 2.343(3) Å) is longer than the distance between the platinum and the chlorine atom *trans* to the helicene (Pt-Cl2: 2.291(3) Å). These values are in full agreement with literature data from similar complexes,[8] and with the stronger effect of phosphine compared to pyridine-type ligands. In the complex, the helicity of the helicene ligand is 46.46° and is therefore comparable to the helicity of the free 4-aza[5]helicene ligand (51.13°, see ref. 6), suggesting that no ligand distortion occurs upon metal coordination.

Interestingly, the trapped dichloromethane molecules, sitting in the inversion center, form weak C-H···Cl interactions with the first ring of the helicene and with one phenyl ring of the PPh_3 group. Such interactions extend along the *x* crystallographic axis forming a 1D chain (Figure 2a). In addition, intermolecular C-H···π (Figure 2b) and inter/intramolecular π–π interactions (Figure 2c) can be observed between the phenyl rings of the PPh_3 ligand and either the central or the terminal aromatic rings of the poly-fused helicene backbone, within two heterochiral complexes formed by *M*- and *P*-4-aza[5]helicene ligands. Note however that in solution the aza[5]helicenes are known to be configurationally unstable.[6]

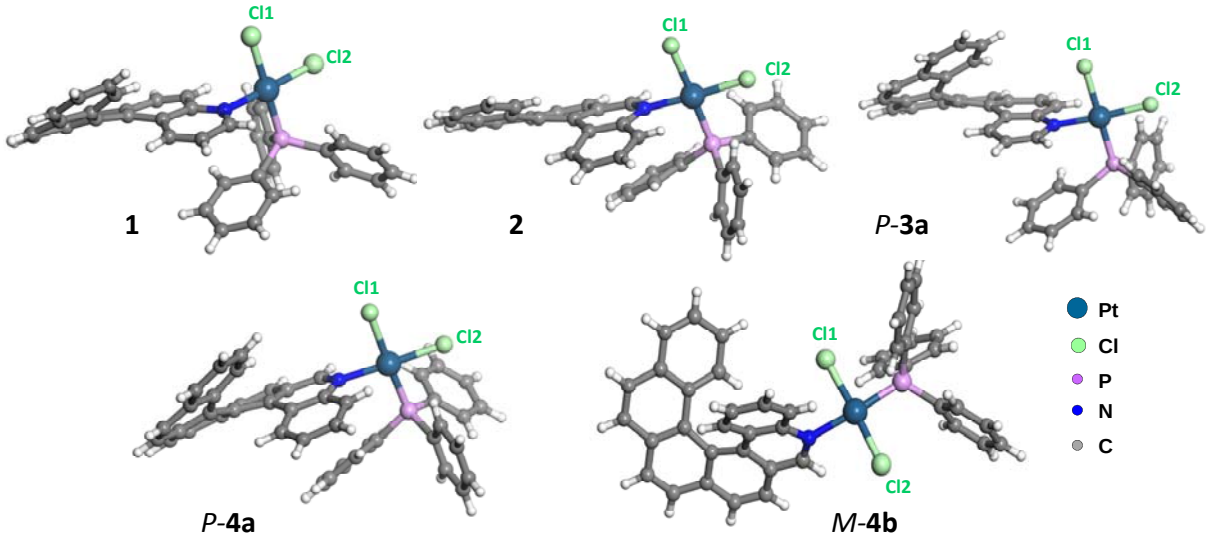

Figure 1. X-ray crystallographic structures of *cis* Pt-complexes **1, 2, 3a, 4a** and *trans* Pt-complex *M*-**4b**.

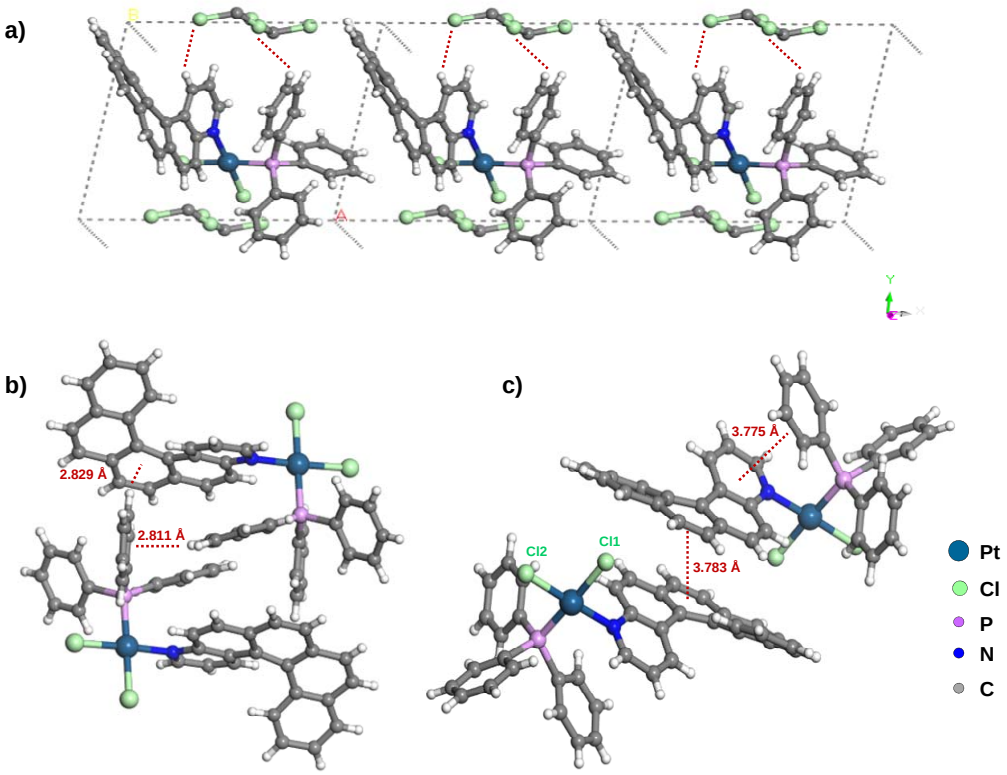

Figure 2. Crystal structure of **1** showing a) the arrangement along the x axis, with H-bonding interactions involving the CH_2Cl_2 solvent molecules (disordered, two positions found), b) the intermolecular CH-π interactions and c) the inter/intramolecular π-π interactions between PPh_3 and the pyridyl cycle, and between the two central rings of two **4H5** in the heterochiral assembly of *cis*-$PtCl_2$(**4H5**)(PPh_3) (**1**) .

Complex **2** crystallizes in the monoclinic space group *C*2/*c*. Owing to the centrosymmetric nature of the space group, molecules with opposite *M* and *P* handedness are present in the unit cell (Figure 3). This complex is characterized by the presence of a network of interactions whereby each molecule (A) is linked to three others (B, C, D) by two types of hydrogen bonds. These can be classified as horizontal links (see, for instance, Cl1(A)…H8(B) and Cl3(C)…H8(A) of Figure 3a) and vertical links (see Cl1(A)…H6(D) and Cl2(D)…H6(A) in

Figure 3a). The latter seem to suggest a cooperative effect between molecules A and D. Moreover, π-π interactions are sketched in Figure 3b. Intramolecular π-π stacking can be observed between the aromatic ring of the phosphine and the azahelicene ligands on the same metal complex, while intermolecular π-π interactions occur between helicene ligands from different metal complexes, with the interacting molecules showing the same chirality (either *M* or *P*).

Overall, the *cis* arrangement of the chlorine ligands in Pt complexes **1** and **2** demonstrates that the stereochemistry is maintained during the replacement of propionitrile by the 4- or 5-aza[5]helicene ligands **4H5** and **5H5**. Indeed, Belli Dell'Amico *et al.* observed that the *cis* isomer **5a** is more stable that the *trans* isomer (*trans*-**5b**, *vide infra*) in a propionitrile solution at room temperature.[9]

Cis and *trans* Pt-complexes of aza[6]helicenes

The synthesis of 4- and 5-aza-[6]helicene Pt complexes **3a**,**b** and **4a**,**b** from **4H6**[10] and **5H6**[11] was accomplished by a different strategy. It was indeed observed that the nitrile substitution reaction at RT was very slow, whereas the reaction would occur overnight upon heating. Indeed, the use of non-nitrile based solvents with a sufficiently high boiling point, e.g., toluene, promoted complex formation. The reaction was monitored by ^{31}P-NMR, which showed the complete disappearance of the starting reactants and the onset of new signals at different chemical shifts and with different *J* couplings. The detailed characterization of the reaction product was obtained by ^{1}H-NMR and ESI mass spectrometry (see ref. 4 and SI).

a)

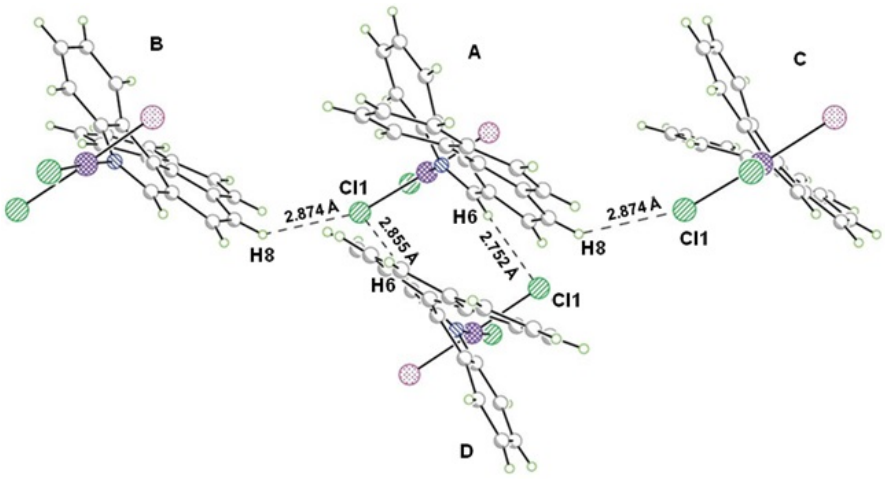

b)

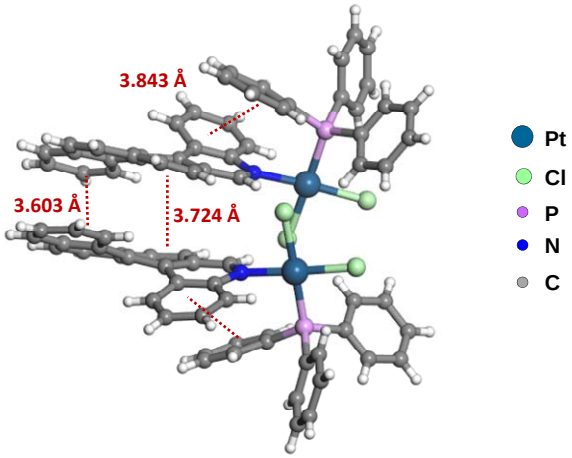

Figure 3. Intermolecular interactions in *cis*-$PtCl_2(5H5)(PPh_3)$ **2**: hydrogen bonds (a), π-π interactions between aromatic part of the complexes (b).

Previous studies[9] demonstrated that in the *cis*-**5a** complex the nitrile group can easily be substituted by another ligand in refluxing toluene. The substitution is achieved via isomerization to the *trans* complex **5c**– which is more reactive than the *cis* one likely because of the *trans*-

effect of the phosphine ligand – and the possible formation of the chlorido-bridged *trans*-[PtCl(μ-Cl)(PPh_3)]$_2$ dimer *trans*-**5c** (Scheme 3). The latter can then be opened by many ligands in a relatively straightforward way.[12] Moreover, the presence of the phosphorus atom in the triphenylphosphine ligand allows the use of ^{31}P-NMR as a fast and unambiguous structural characterization method. Indeed, complex formation could be followed over time by monitoring the variation of the ^{31}P chemical shifts and heteronuclear *J* couplings.

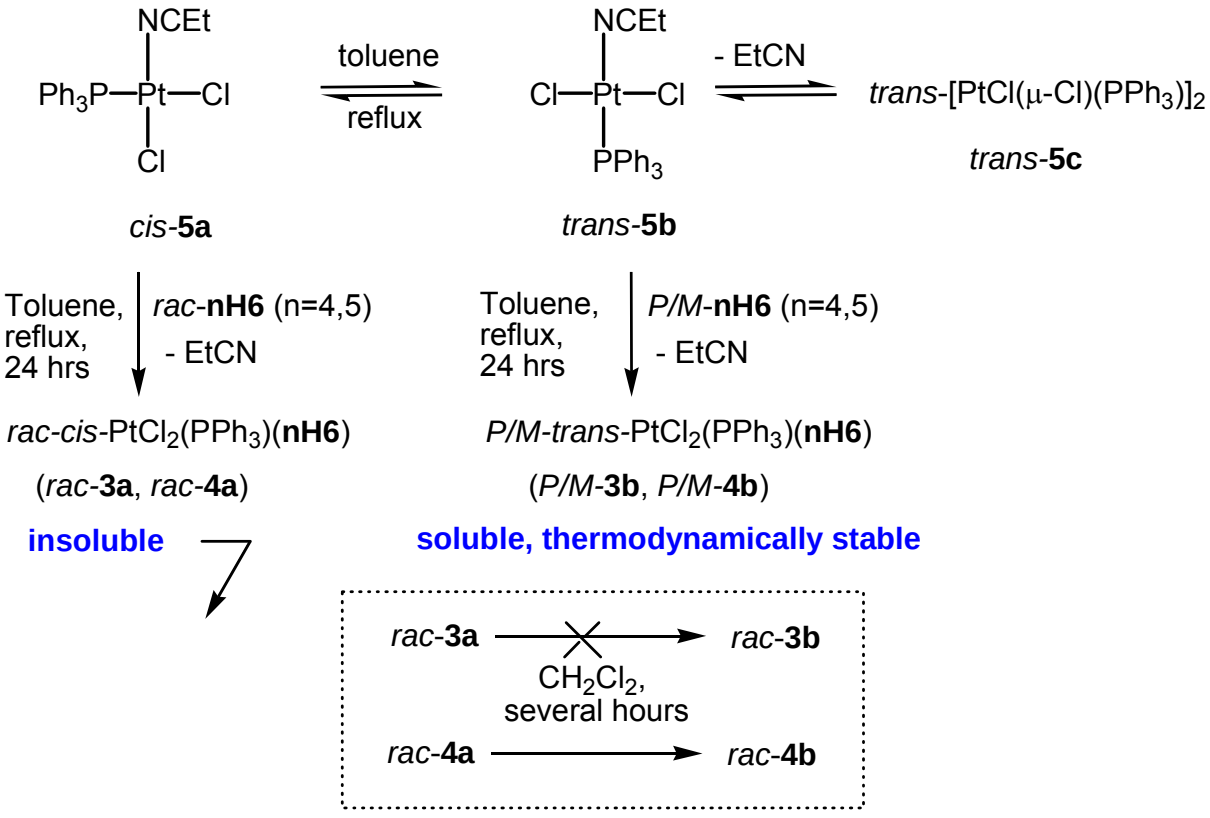

Scheme 3. Generic reaction pathway for 4- and 5-aza[6]helicene-platinum complexes with either *cis* (**3a**, **4a**) or *trans* (**3b**, **4b**) stereochemistry. Equilibrium process of platinum precursor as a mixture of *cis*-**5a**, *trans*-**5b** and μ-chlorido bridged *trans*-**5c**.

We have previously reported that the reaction of racemic 4-aza[6]helicene **4H6** with *cis*-$PtCl_2(NCEt)PPh_3$ **5** in refluxing toluene for one night resulted in the precipitation the *cis*-isomeric complex **3a** while the reaction of enantiopure *P*- and *M*-**4H6** under the same conditions yielded the enantiopure *trans*-isomeric complex *P*- and *M*-**3b**. This surprising result was identified as a dynamic process, namely a crystallization-induced diastereoselective transformation, due to the different solubilities of racemic and enantiopure 4-aza[6]helicene Pt complexes that displace the *cis*-*trans* equilibrium of Pt-precursors **5a-c** in refluxing toluene (see Scheme 3).[4] As already described in ref. 4, complex **3a** crystallizes in the triclinic *P*-1 space group with the presence of *M* and *P* 4-aza[6]helicenes. The geometry around the platinum atom is square planar (Figure 1). The central metal is coordinated by two chlorine ligands in a *cis* mutual position, one 4-aza[6]helicene ligand and one PPh_3 group. Weak intramolecular π-π interactions were found to occur between one phenyl ring of PPh_3 and the pyridyl ring (centroid-centroid distance 3.852 Å) and a set of hydrogen bonds involving the Cl ligands through the whole crystalline network.

Following the uncommon behavior of **4H6** towards Pt complexation, we set out to investigate whether the same results could be observed with similar ligands such as **5H6**. Indeed, using the same procedure with racemic **5H6**, *i.e.*, reacting it with *cis*-**5a** in refluxing toluene overnight, resulted in the precipitation of a yellow solid that was identified as the *cis*-Pt complex **4a** (*vide infra*). In this new complex, differences in the ^{1}H chemical shifts between the non coordinated and the coordinated **5H6** ligand could be observed. For example, the H2 and H15 protons appeared as ddd signals at 6.62 and 6.73 ppm in complex **4a** while they resonate at the same chemical shift (6.8 ppm) in the free **5H6** ligand. The H6 proton is greatly influenced by the metal coordination and appears as an up-field shifted singlet at 9.16 ppm with a ^{195}Pt-H coupling

constant of 45 Hz. The ^{31}P NMR spectrum of **4a** shows a single signal at 6.9 ppm, with a ^{195}Pt-P coupling constant of 3850 Hz, very similar to the one observed for complex **3a** (see SI).

On the contrary, when using enantiopure *P*- or *M*-**5H6** and under the same reaction conditions, the enantiopure *P*- or *M*-*trans*-Pt complexes **4b** were obtained in reasonably good yields. These new *trans* complexes were first characterized by ^{31}P NMR which displayed signals that were different from complex **4a** (2.8 ppm, $^{1}J_{\text{P-Pt}}$ = 3645 Hz, see SI). Similarly, the ^{1}H-NMR spectrum displayed signals at different chemical shifts than **4a** and was finally identified as the *trans*-isomeric complex by X-ray crystallography (*vide infra*). Clearly, these results show that **5H6** displays the same behavior as **4H6**, the reactivity being triggered by the enantiopurity of the starting helicene ligand (racemic *vs.* enantiopure) and corresponding to a crystallization-induced diastereoselective transformation. To our knowledge, this is a very uncommon behavior in helicenes coordination chemistry.

Note however that the *cis* Pt complexes **3a** and **4a** display different behaviors in CH_2Cl_2 solutions. It was in fact observed by ^{1}H NMR spectroscopy and electronic circular dichroism (*vide infra*) that *rac*-**4a** slowly isomerizes to the more thermodynamically stable complex *rac*-**4b** after several hours, while *rac*-**3a** remains unchanged. For this reason, the isolation of enantiopure samples of the *cis* complex **4a** by HPLC separation over a chiral stationary phase is unattainable, as well as ^{195}Pt and ^{13}C NMR spectra of reasonably good quality. At this stage it is interesting to note that **3a** appears more stable than **4a** since the latter isomerizes to **4b** while complex **3a** remains unchanged in solution. Theoretical calculations have recently emphasized the role of π–π interactions between the PPh_3 ligand and the 4aza[6]helicene in stabilizing some conformations of **3a**. It is therefore most probable that the π–π interactions taking place in **4a** are not sufficient for stabilizing the *cis* configuration.[13]

Despite its low solution stability and easy transformation to *trans* complex **4b**, single crystals of *rac*-**4a** were obtained and characterized by X-ray crystallography. Complex **4a** crystallizes in the triclinic space group *P*-1. Its X-ray crystallographic structure, depicted in Figures 1 and 4, reveals a square planar geometry around the platinum atom which is coordinated by two chlorine ligands in a *cis* mutual position, one 5-aza[6]helicene ligand and one PPh_3. Owing to steric hindrance, a small distortion from the ideal 90° geometry is observed (the N5-Pt-P and N5-Pt-Cl1 angles are 94.27(17)° and 86.46(7)°, respectively). As for complex **3a**, the distance between the platinum atom and the chlorine atom *trans* to the phosphine ligand (Pt-Cl1: 2.349(2) Å) is longer than the distance between the platinum atom and the chlorine atom *trans* to the helicene ligand (Pt-Cl2: 2.2933(16) Å). Interestingly, weak intramolecular π–π interactions take place between one phenyl of the PPh_3 ligand and the pyridyl ring (centroid-centroid distance 3.774 Å). As discussed for **3a**, owing to the steric hindrance of the helicene moiety, the PPh_3 is stacked on one side of the pyridyl ring, thus generating planar chirality, with the $pyPtCl_2$ defining the chiral plane.[4,14] Indeed, C6-N-Pt-P and C4a-N-Pt-Cl1 torsion angles of -79.63 and -87.38° (p*M*-chirality)[£] are measured in the *cis*-**4a** molecule having the *M*-4-aza[6]helicene ligand, suggesting that the *M*-helicity induces a fixed p*M*-chiral planar sense.[4] The crystal packing is arranged to form parallel layers on the *yz* plane, as shown in Figure 4. The individual layers are connected by hydrogen bonds (distances 2.8-2.9 Å) of the type Cl2···H11 (helicene) and Cl1···H^o (PPh_3) shown in Figure 4 in horizontal and vertical projection, respectively. Heterochiral assemblies are also found thanks to π–π interactions between azahelicenes of opposite handedness (Figure 5a). Finally, the crystal packing of **4a** reveals a set of several different intermolecular CH···Cl hydrogen bonds that contribute to lattice stabilization (Figure 5b).

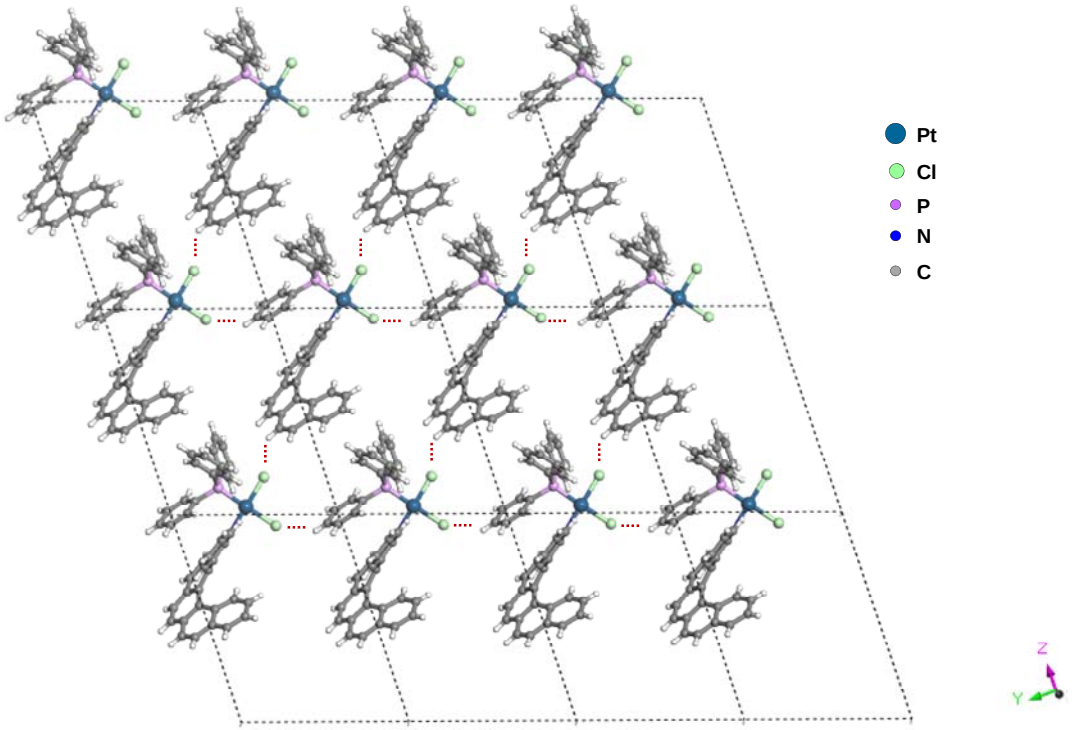

Figure 4. Arrangement of *cis* complex **4a** in the *yz* plane. Hydrogen bonds between Cl and H atoms are emphasized in red.

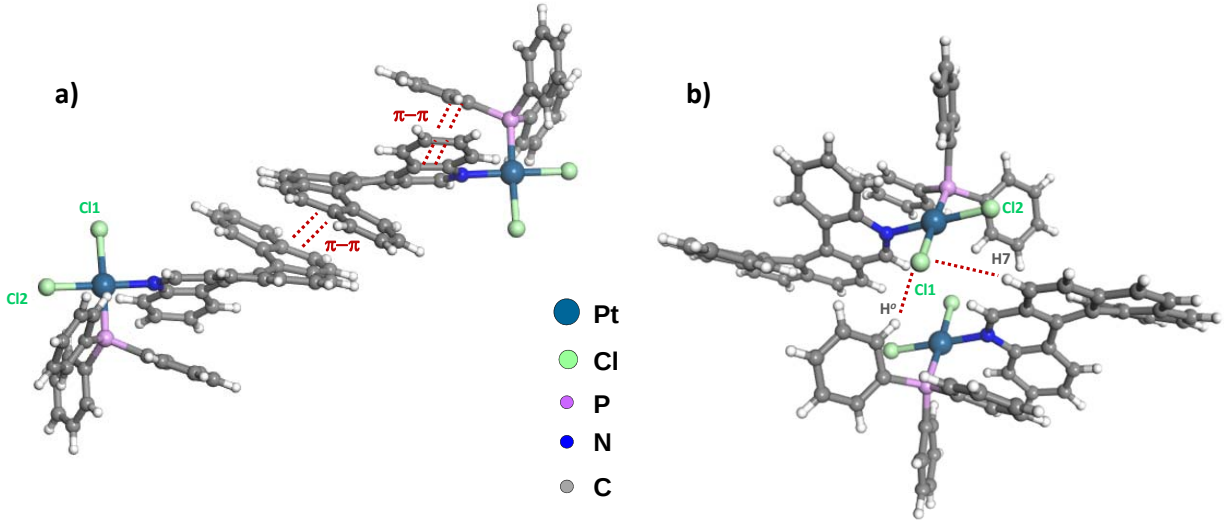

Figure 5. a) π-π interaction between helicenic rings of two adjacent heterochiral *P*- and *M*-**4a**. b) Selected Cl···H interactions between two heterochiral *P*- and *M*-**4a**.

Single crystals of enantiopure *M*-**4b** could be grown and characterized by X-ray crystallography. Complex *M*-**4b** crystallizes in the orthorhombic chiral space group $P2_12_12_1$, with one molecule in the asymmetric unit and four molecules in the unit cell. While the Pt center shows an almost undistorted square planar geometry (Figures 1 and 6) (angles N-Pt-P: 170.70(11)°, Cl1-Pt-Cl2: 174.67(5)°, N-Pt-Cl1: 86.67(11)°, N-Pt-Cl2: 90.48(11)°), the two chlorine atoms are now in a mutual *trans* configuration. As a result, the two Pt-Cl bond distances are similar (Pt-Cl1: 2.3121(11) Å, Pt-Cl2: 2.2823(11) Å). A helicity angle[#] of 53.66° was measured in the solid state, showing that no ligand distortion occurs upon complexation. Several H···Cl hydrogen bonds are found between neighboring molecules (Cl2···H4: 2.707 Å, Cl1···H10: 2.932 Å, Cl2···H^m(PPh_3): 2.968 Å, Cl2···H^p(PPh_3): 3.163 Å) (see Figures 6a,b).

The electronic circular dichroism (ECD) spectra of the enantiopure samples of *M*- and *P*-**4b** were also measured (Figure 7). The mirror-image ECD spectra display the characteristic bands of helicene derivatives, and are very similar to the ECD spectra of the **5H6** ligand,[10] showing that in this case the coordination to $PtCl_2(PPh_3)$ moiety has no influence on the chiroptical properties of the complexes.

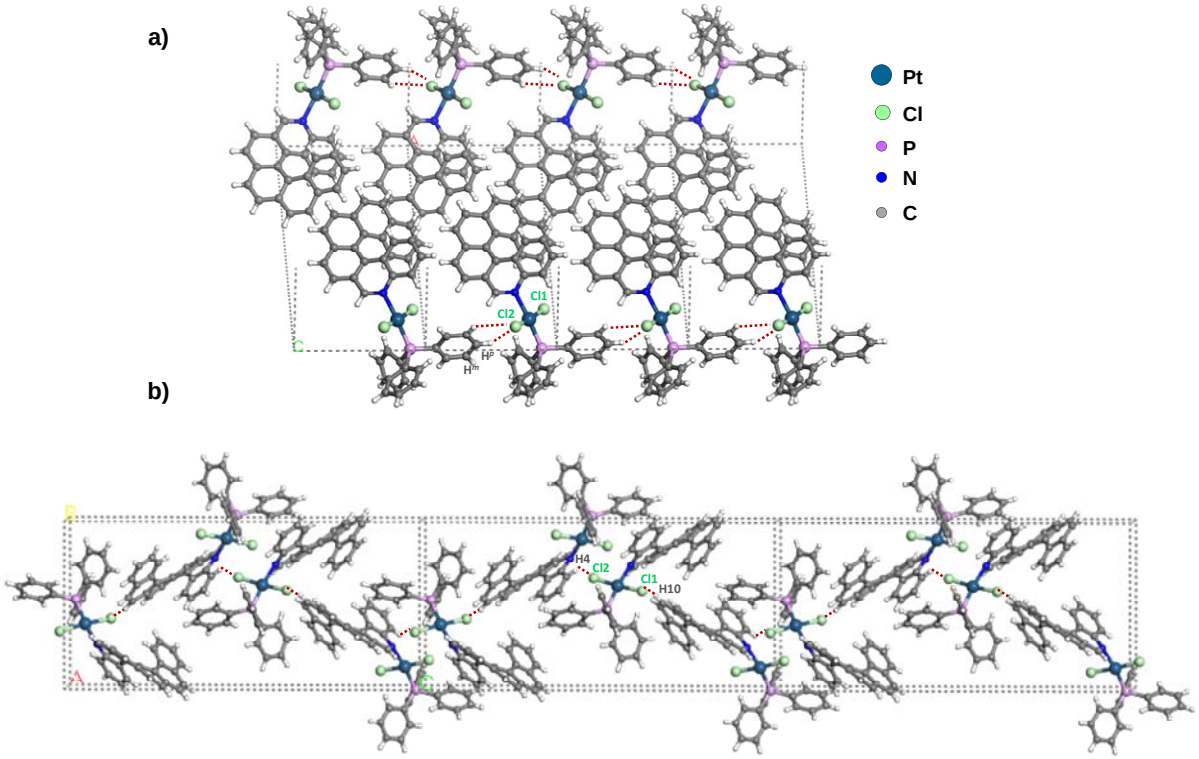

Figure 6. Arrangement of *trans* complex **4b** a) in the xz plane and b) in the *yz* plane. Hydrogen bonds between Cl and H atoms are emphasized in red.

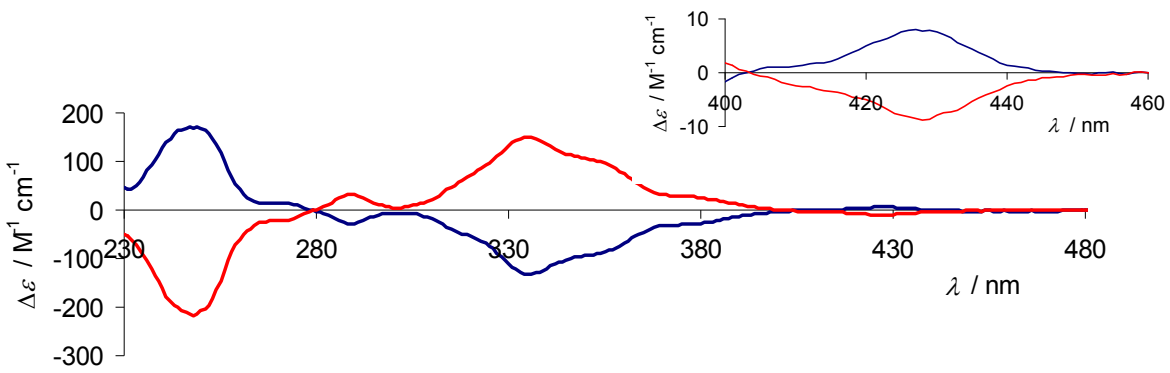

Figure 7. Mirror-image ECD spectra of *P* (red) and *M* (blue) *trans* Pt complexes **4b** (CH_2Cl_2, 5 10^{-5} M). Insert: Magnified ECD bands in the 400-460 nm region.

Conclusions

We have reported the synthesis and the structural characterization of a number of novel *cis* and *trans* azahelicene/metal complexes using 5- and 6-membered helicenes with the N atom in position 4 and 5. The very different packing arrangements shown by these complexes is modulated by the different position of the nitrogen atom in the helicene moiety. While square planar (SP-4) Pt(II) complexes of general formula LL'PtX2 displaying the usual *cis*/*trans* isomerism is well-known in coordination chemistry,[15] the effect of either the racemic or the enantipure forms of aza[6]helicenes on such stereochemistry is an uncommon phenomenon.[4] Such isomerism can have important practical implications in biology as with $Pt(NH_3)_2Cl_2$ (*cis*-platin) which is an efficient antitumor drug, while its *trans* isomer is ineffective.[16a,b] Therefore, the control of the stereochemistry of SP-4 platinum complexes may provide an efficient tool for the development of anticancer drugs[16] as well as the design of innovative molecular materials for optical applications.[1h]

General

Toluene and diethylether were freshly distilled under argon from appropriate drying agent. All other reagents and solvents were bought from Sigma-Aldrich and used either as such or after drying where required. All complexation reactions were done under argon using standard Schlenk techniques. NMR spectra ^{1}H and ^{31}P were recorded at room temperature on a Bruker Avance 500 spectrometer equipped with a QNP switchable probe ^{13}C-^{31}P-^{19}F-^{1}H and operating at proton resonance frequency of 500 MHz. Chemical shifts are reported in parts per million (ppm) relative to Me_4Si as external standard; coupling constants are expressed in Hz. ^{31}P-NMR downfield chemical shifts are expressed with a positive sign, in ppm, relative to external 85% H_3PO_4. ^{195}Pt-NMR spectra were performed on a Bruker DRX 500 spectrometer, equipped with a BBI broadband probe; spectra were referenced to a solution of H_2PtCl_6 in D_2O. Some of the samples were measured by the CRMPO - Rennes.

All spectra were obtained using deuterated dichloromethane or chloroform as solvents. The terms s, d, t, q, m indicate respectively singlet, doublet, triplet, quartet, multiplet; b is for broad, dd is doublet of doublets, ddd is doublet of doublets of doublets, AB is the AB spin system. Positive-ion ESI-MS was performed on Esquire 3000 plus ion-trap mass spectrometer (Bruker Daltonik, Bremen, Germany) equipped with an ESI source. Sample solutions were introduced into the ion source at a flow-rate 4 μL m^{-1}, capillary voltage 3.8 kV, drying gas temperature 250 °C, drying gas flow rate 5 L m^{-1}, nebulizer pressure 14 psi. Nitrogen was used as both nebulizing gas and drying gas. Specific rotations (in deg cm^2g^{-1}) were measured in a 1 dm thermostated quartz cell on a Perkin Elmer-341 polarimeter. Circular dichroism (in $M^{-1}cm^{-1}$) was measured on a Jasco J-815 Circular Dichroism Spectrometer (Biosit platform - Rennes). *cis*-$PtCl_2(NCEt)(PPh_3)$ complex **5a**,[9] 4-aza[6]helicene **4H6**[10] and 5-aza[6]helicene **5H6**[11] were prepared according to literature procedures. The synthesis of complexes **3a**,**b** was described elsewhere.[4]

CCDC numbers: 1421169 (**1**), 1421176 (**2**), 940838 (*rac*-**3a**), 947611 (*rac*-**4a**), 1062437 (*M*-**4b**).

Syntheses

Cis-$PtCl_2(PPh_3)$(4H5): complex 1

A 50 mL Schlenk tube was loaded with *cis*-$PtCl_2$(NCEt)(PPh_3) (50 mg, 0.086 mmol), 4-aza[5]helicene **4** (24 mg, 0.086 mmol) and propionitrile (5 mL). The mixture was stirred at room temperature for 4 days, then dried under vacuum and washed several times with Et_2O. 59 mg of yellow solid were recovered (85 % yield) and identified as the product. Single crystals were obtained by slow evaporation of a dichloromethane solution. ^{1}H NMR ($CDCl_3$, 500 MHz): δ 9.65 (d, $^3J_{H\text{-}H}$ = 8.7, 1H, *H5*); 9.21 (ddd, $^3J_{H\text{-}H}$ = 8.5,1H, *H3*); 9.01 (dd, $^2J_{H\text{-}H}$ = 8.2 Hz, 1H, *H1*); 8.39 (dd, $^2J_{H\text{-}H}$ = 8.7 Hz, 1H, *H14*); 8.28 (d, $^2J_{H\text{-}H}$ = 9.2 Hz, 1H, *H6*); 7.97–7.85 (m, 11H, *H7/H8/H9/H10/H11, PPh$_3$*); 7.55–7.35 (m, 11H, *H12/H13*, *PPh$_3$*); 7.28 (ddd, 1H, *H2*). ^{31}P NMR ($CDCl_3$, 202 MHz): 3.1, $^1J_{P\text{-}Pt}$ = 3670 Hz. ^{195}Pt NMR ($CDCl_3$, 107 MHz): −3625 (d), $^1J_{Pt\text{-}P}$ = 3670 Hz.

Cis-$PtCl_2(PPh_3)$(5H5): complex 2

A 50 mL Schlenk tube was loaded with *cis*-$PtCl_2$(NCEt)(PPh_3) (50 mg, 0.086 mmol), 5-aza[5]helicene **5** (29 mg, 0.104 mmol) and propionitrile (8 mL). The mixture was stirred at room temperature for 1 night. The product precipitates as a yellow powder, to afford 35 mg of product (43 % yield). The solid was crystallized from CH_2Cl_2/heptane. ^{1}H NMR ($CDCl_3$, 500 MHz): 9.77 (d, $^3J_{H\text{-}P}$ = 4.2, 1H, *H6*); 9.66 (dd, $^3J_{H\text{-}H}$ = 8.3, $^4J_{H\text{-}H}$ = 1.0, 1H, *H4*); 8.52 (dd, $^3J_{H\text{-}H}$ = 8.7, $^4J_{H\text{-}H}$ = 0.8, 1H, *H14*); 8.50 (dd, $^3J_{H\text{-}H}$ = 9.8, $^4J_{H\text{-}H}$ = 0.7, 1H, *H1*); 8.04 (d, $^3J_{H\text{-}H}$ = 8.2, *H8*); 8.01 (d, $^3J_{H\text{-}H}$ = 9.1, 1H, *H9/H10*); 7.99 (d, $^3J_{H\text{-}H}$ = 8.2, 1H, *H7)*; 7.95 (dd, $^3J_{H\text{-}H}$ = 8.1, $^4J_{H\text{-}H}$ = 1.2, 1H, *H11*); 7.91–7.86 (m, 6H, *PPh3*); 7.80 (ddd, $^3J_{H\text{-}H}$ = 8.4, 7.0, $^4J_{H\text{-}H}$ = 1.4 1H, *H3*); 7.56 (ddd, $^3J_{H\text{-}H}$ = 8.0, 6.7, $^4J_{H\text{-}H}$ = 1.1 1H, *H12*) 7.48–7.44 (m, 9H, *PPh3*); 7.35 (ddd, $^3J_{H\text{-}H}$ = 8.1, 6.7, $^4J_{H\text{-}H}$ = 1.1 1H, *H13*); 7.32 (ddd, $^3J_{H\text{-}H}$ = 8.4, 7.0, $^4J_{H\text{-}H}$ = 1.4 1H, *H2*). ^{31}P NMR ($CDCl_3$, 202 MHz): 3.1, $^1J_{P\text{-}Pt}$ = 3660 Hz. ^{195}Pt NMR ($CDCl_3$, 107 MHz): −3522 (d), $^1J_{Pt\text{-}P}$ = 3660 Hz.

Cis-$PtCl_2(PPh_3)$(5H6): complex 4a

The synthetic procedure for this complex is the same reported above, using 5-aza[6]helicene **15** as ligand. We obtained a yellow solid as product, with a yield of 69%. The product was

crystallized from a CH_2Cl_2/$^{i}Pr_2O$ mixture. ^{1}H NMR (CD_2Cl_2, 500 MHz): 9.44 (dd, $^{3}J_{H\text{-}H}$ = 8.5, $^{4}J_{H\text{-}H}$ = 1.1, 1H, *H4*); 9.16 (s, $^{3}J_{H\text{-}Pt}$ = 45, 1H, *H6*); 8.08 (AB, $^{3}J_{H\text{-}H}$ = 8.4, 1H, *H8*); 7.98-7.86 (m, 4H, H9/H10/H11/H12); 7.79 (dd, $^{3}J_{H\text{-}H}$ = 8.1 Hz, $^{4}J_{H\text{-}H}$ = 1.4, 1H, *H13*); 7.56 (dd, $^{3}J_{H\text{-}H}$ = 8.9, $^{4}J_{H\text{-}H}$ = 0.8 Hz, 1H, *H16*); 7.52-7.47 (m, 6H, *H PPh$_3$*); 7.32 (AB, $^{3}J_{H\text{-}H}$ = 8.4, 1H, *H7*); 7.30 (ddd, $^{3}J_{H\text{-}H}$ = 8.5, 6.9, $^{4}J_{H\text{-}H}$ = 1.4, 1H, *H3*); 7.25 (dd, $^{3}J_{H\text{-}H}$ = 8.4, $^{4}J_{H\text{-}H}$ = 1.3 Hz, 1H, *H1*); 7.21 (ddd, $^{3}J_{H\text{-}H}$ = 8.1, 6.9, $^{4}J_{H\text{-}H}$ = 1.2, 1H, *H14*); 7.14-7.10 (m, 3H, *H PPh$_3$*); 7.06–7.02 (m, 6H, *H PPh$_3$*); 6.73 (ddd, $^{3}J_{H\text{-}H}$ = 8.5, 6.9, $^{4}J_{H\text{-}H}$ = 1.4, 1H, *H15*); 6.62 (ddd, $^{3}J_{H\text{-}H}$ = 8.5, 6.9, $^{4}J_{H\text{-}H}$ = 1.4, 1H, *H2*). ^{31}P NMR (CD_2Cl_2, 202 MHz): 6.9, $^{1}J_{P\text{-}Pt}$ = 3853 Hz.

***P-(+) and M-(-)-Trans*-PtCl$_2$(PPh$_3$)(5H6): complex 4b**

A 10 mL Schlenk tube was loaded with *cis*-$PtCl_2$(NCEt)(PPh_3) (17.4 mg, 0.0332 mmol), a little excess of enantiopure 5-aza[6]helicene *P*-(+)-**5H6** (15 mg, 0.0334 mmol) and toluene as solvent (3.0 mL). The mixture was heated under stirring in a sealed tube at 130°C for one night; no precipitation was observed.The yellow solution thus obtained was then completely dried under vacuum, allowing 14.6 mg of compound (59% yield) to be recovered. The same procedure was carried out in parallel using *M*-(-)-**4H6** as the ligand, yielding the *M*-(-)-**4b** complex, as confirmed by NMR experiments. ^{1}H NMR (CD_2Cl_2, 400 MHz): δ 9.88 (d, $^{4}J_{H\text{-}H}$ = 4.2, $^{3}J_{H\text{-}Pt}$ = 24 Hz, 1H, *H6*), 9.52 (d, $^{3}J_{H\text{-}H}$ = 8.4, 1H, *H4*), 8.23 (m, 2H), 8.19 (d, $^{3}J_{H\text{-}H}$ = 8.3, 1H), 8.19 (d, $^{3}J_{H\text{-}H}$ = 8.3, 1H), 8.09 (d, *J* = 8.7, 1H), 8.03 (d, $^{3}J_{H\text{-}H}$ = 8.7, 1H), 8.00 (d, $^{3}J_{H\text{-}H}$ = 8.7, 1H), 7.96 - 7.87 (m, 7H), 7.58 (m, 1H, *H3*), 7.62 - 7.52 (m, 11H), 7.29 (unres. t, $^{3}J_{H\text{-}H}$ = 7.4, 1H, H14), 6.82 (unres. t, $^{3}J_{H\text{-}H}$ = 7.7, 1H, H2), 6.77 (unres. t, $^{3}J_{H\text{-}H}$ = 7.7, 1H, H15). ^{13}C NMR (126 MHz, CD_2Cl2) δ 155.89 (*C*H), 142.63 (*C*), 136.89 (*C*), 135.57 (*C*Hx3), 135.48 (*C*Hx3), 132.99 (*C*), 132.71 (*C*), 132.62 (*C*), 131.53(*C*H), 131.51 (*C*Hx2), 131.16 (*C*H), 129.72 (*C*), 129.66 (*C*H), 129.61 (*C*), 129.58 (*C*H), 129.10 (*C*), 128.99 (*C*H), 128.63 (*C*Hx3), 128.59 (*C*H), 128.54 (*C*Hx3), 128.48 (*C*), 128.43 (*C*H), 128.37 (*C*H), 127.41 (*C*H), 127.38 (*C*H), 126.93 (*C*H), 126.57 (*C*H), 126.55 (*C*H), 126.35 (*C*H), 126.19 (*C*H), 126.16 (*C*), 126.03 (*C*), 126.00 (*C*), 122.74 (*C*). ^{31}P NMR (CD_2Cl_2, 162 MHz): 2.8, $^{1}J_{P\text{-}Pt}$ = 3645 Hz. ^{195}Pt NMR ($CDCl_3$, 107 MHz): −3525, $^{1}J_{P\text{-}Pt}$ = 3653 Hz.

X-ray data

The diffraction data for **1** and **2** were recorded at room temperature with a Bruker X8 Prospector APEX-II/CCD diffractometer equipped with a focusing mirror (Cu-K_α radiation, λ = 1.54056 Å). The diffraction data for **3** and **4** were recorded at 150 K with an APEX II Bruker-AXS with Mo-*K*α radiation (λ = 0.71073 Å). The structures were determined using direct methods and refined (based on F2 using all independent data) by full-matrix least-square methods (SHELXTL 97).[17] All non-hydrogen atoms were located from different Fourier maps and refined with anisotropic displacement parameters. Hydrogen atoms were added in riding positions.

ASSOCIATED CONTENT

Supporting Information. Further details on NMR, ESI MS, crystallographic information, HPLC separations can be found in the Supporting Information. This material is available free of charge via the Internet at http://pubs.acs.org.

AUTHOR INFORMATION

Corresponding Authors

Contact information for the author(s) to whom correspondence should be addressed:

jeanne.crassous@univ-rennes1.fr, andrea.mele@polimi.it

Author Contributions

The manuscript was written through contributions of all authors. All authors have given approval to the final version of the manuscript.

Funding Sources

This research was supported by the Ministère de la Recherche et de l'Enseignement Supérieur, the CNRS, and the ANR (12-BS07-0004-METALHEL-01). DM was financed by MIUR Dottorato di Ricerca XXVI ciclo.

Aknowledgments

Elsa Caytan is warmly thanked for her help in measuring ^{195}Pt NMR. The authors wish to thank Walter Panzeri (CNR-ICRM Milano) for technical assistance.

Notes

[$] Increasing the temperature resulted in the formation of side products among which the *trans* complex as observed by ^{31}P NMR and ^{195}Pt NMR. Moreover, the target complexes showed degradation after few days in solution of chlorinated solvents like chloroform and dichloromethane. For this reason, satisfactory ^{13}C NMR spectra could not be obtained.

[#] The helicity is defined as the dihedral angle between the two terminal rings of the helicene derivative.

[£] The p label in p*M* and p*P* is used to differentiate planar from helical chirality.

References

[1] Selected reviews: a) Shen, Y.; Chen, C. -F. *Chem. Rev*. **2012**, *112*, 1463; b) Gingras, M. *Chem. Soc. Rev.* **2013**, *42*, 1051; c) Stará, I. G.; Starý, I. in: Siegel, J. S.; Tobe Y. (Eds.), *Science of Synthesis*, vol. 45, Thieme, Stuttgart, **2010**, pp. 885-953; d) Rajca, A.; Miyasaka, M. in: Müller, T. J. J.; Bunz U. H. F. (Eds.), *Functional Organic Materials* Wiley-VCH, Weinheim, **2007**, pp. 543-577; e) Urbano, A. *Angew. Chem. Int. Ed*. **2003**, *42*, 3986; f) Katz, T. J. *Angew. Chem. Int. Ed*. **2000**, *39*, 1921; g) Martin, R. H. *Angew. Chem. Int. Ed.* **1974**, *13*, 649; h) Saleh, N.; Shen, C.; Crassous, J. *Chem. Sci.* **2014**, *5*, 3680; i) Bosson, J.; Gouin, J.; Lacour, J. *Chem. Soc. Rev.* **2014**, *43*, 2824; j) Aillard, P.; Voituriez, A.; Marinetti, A. *Dalton Trans.* **2014**, *43*, 15263.

[2] a) Crassous J. *Chem. Soc. Rev.* **2009**, *38*, 830; b) Crassous, J. *Chem. Comm*. **2012**, *48*, 9684.

[3] Selected: a) Honzawa, S.; Okubo, H.; Anzai, S.; Yamaguchi, M.; Tsumoto, K.; Kumagai, I.; *Bioorg. Med. Chem.* **2002**, *10*, 3213; b) Passeri, R.; Aloisi, G. G.; Elisei, F.; Latterini, L.; Caronna, T.; Fontana, F.; Natali Sora, I. *Photochem. Photobiol. Sci.* **2009**, *8*, 1574; c) Xu, Y.; Zhang, Y. X.; Sugiyama, H.; Umano, T.; Osuga, H.; Tanaka, K. *J. Am. Chem. Soc.* **2004**, *126*, 6566; d) Shinohara, K.; Sannohe, Y.; Kaieda, S.; Tanaka, K.; Osuga, H.; Tahara, H.; Xu, Y.; Kawase, T.; Bando, T.; Sugiyama, H. *J. Am. Chem. Soc.* **2010**, *132*, 3778; e) Kel, O.; Fürstenberg, A.; Mehanna, N.; Nicolas, C.; Laleu, B.; Hammarson, M.; Albinsson, B.; Lacour, J.; Vauthey, E. *Chem. Eur. J.* **2013**, *19*, 7173; f) Tsuji, G.; Kawakami, K.; Sasaki, S. *Bioorg. Med. Chem.* **2013**, *21*, 6063.

[4] Mendola, D.; Saleh, N.; Vanthuyne, N.; Roussel, C.; Toupet, L.; Castiglione, F.; Caronna, T.; Mele, A.; Crassous, J. *Angew. Chem. Int. Ed*. **2014**, *53*, 5786.

[5] Jacques, J.; Collet, A.; Wilen, S. H. *Enantiomers, Racemates, & Resolutions*, J. Wiley & Sons, New York, **1981**.

[6] Bazzini, C.; Brovelli, S.; Caronna, T.; Gambarotti, C.; Giannone, M.; Macchi, P.; Meinardi, F.; Mele, A.; Panzeri, W.; Recupero, F.; Sironi, A.; Tubino, R. *Eur. J. Org. Chem.* **2005**, 1247.

[7] Kukushkin, V. Y. *Platinum Metals Rev*. **1998**, *42*, 106.

[8] a) Fanizzi, F. P.; Lanfranchi, M.; Natile, G.; Tiripicchio, A. *Inorg. Chem.* **1994**, *33*, 3331; b) Belli Dell'Amico, D.; Broglia, C.; Labella, L.; Marchetti, F.; Mendola, D.; Samaritani, S. *Inorg. Chim. Acta* **2013**, *395*, 181; c) Belluco, U.; Bertani, R.; Meneghetti, F.; Michelin, R. A.; Mozzon, M.; Bandoli, G.; Dolmella, A. *Inorg. Chim. Acta* **2000**, *300-302*, 912.

[9] Belli Dell'Amico, D.; Labella, L.; Marchetti, F.; Samartini, S. *Dalton Trans*. **2012**, *41*, 1389.

[10] Martin, R. H.; Deblecker, M. *Tetrahedron Lett.* **1969**, *41*, 3597.

[11] Abbate, S.; Longhi, G.; Lebon, F.; Castiglioni, E.; Superchi, S.; Pisani, L.; Fontana, F.; Torricelli, F.; Caronna, T.; Villani, C.; Sabia, R.; Tommasini, M.; Lucotti, A.; Mendola, D.; Mele, A.; Lightner, D. A. *J. Phys. Chem. C* **2014**, *118*, 1682.

[12] Jain, V. K.; Jain, L. *Coord. Chem. Rev.* **2005**, *249*, 3075.

[13] Mendola, D.; Famulari, A.; Crassous, J.; Saleh, N.; Caronna, T.; Trotta, F.; Meille, S. V.; Panzeri, W.; Mele, A. *J. Photochem. Photobiol.* A: Chemistry, *submitted*.

[14] a) von Zelewsky, A. *Stereochemistry of Coordination Compounds*, J. Wiley&Sons, Chichester, **1996**; b) Amouri, A.; Gruselle, M. *Chirality in Transition Metal Chemistry: Molecules, Supramolecular Assemblies and Materials*, Wiley-VCH, **2009**; c) Sokolov, V. I. *Chirality and Optical Activity in Organometallic Compounds*, Gordon and Breach Science Publishers, **1990**.

[15] a) Crabtree, R. H. *The organometallic chemistry of the transition metals*, Wiley Interscience, **2005** (4th edition); b) Melnik, M.; Holloway, C. E. *Coord. Chem. Rev.* **2006**, *250*, 2261; c) Wilson, J. J.; Lippard, S. J. *Chem. Rev.* **2014**, *114*, 4470.

[16] a) Lippert, B. *Coord. Chem. Rev*. **1999**, *182*, 263; b) Guo, Z.; Sadler, P. J. *Angew. Chem. Int. Ed.* **1999**, *38*, 1512; c) Ho, C. L.; Wong, W. Y. *Coord. Chem. Rev*. **2013**, *257*, 1614; d) Johnstone, T. C.; Lippard, S. J. *J. Am. Chem. Soc.* **2014**, *136*, 2126.

[17] a) Sheldrick, G. M. *SHELXTL Reference Manual*, Siemens Analytical X-ray Systems, Inc., Madison, Wisconsin, USA **1996**; b) Sheldrick, G. M. *Acta Cryst*. **2008**, *A64*, 112.